Journal of
Applied Crystallography
ISSN 0021-8898
Editor: **Anke R. Kaysser-Pyzalla**

A new Guinier–Porod model

Boualem Hammouda

J. Appl. Cryst. (2010). **43**, 716–719

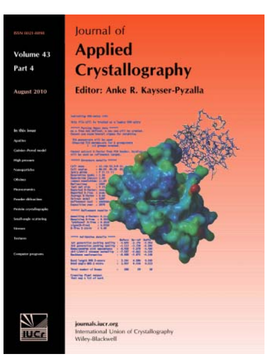

Journal of
Applied
Crystallography
ISSN 0021-8898

Received 9 November 2009
Accepted 28 April 2010

A new Guinier–Porod model

Boualem Hammouda

National Institute of Standards and Technology, Center for Neutron Research, 100 Bureau Drive, Gaithersburg, MD 20899-6102, USA. Correspondence e-mail: hammouda@nist.gov

Small-angle scattering (SAS) curves are characterized by two main features: the Guinier region and the Porod region. Standard linear plots are available to fit SAS data and obtain a radius of gyration and a Porod exponent. A new Guinier–Porod empirical model is introduced to fit SAS data from spherical as well as nonspherical objects such as rods or platelets. It also applies to shapes intermediate between spheres and rods or between rods and platelets. The new model is used to fit SAS data from a Pluronic solution that sequentially forms unimers, then spherical micelles, then cylindrical micelles, then lamellar micelles upon heating. This single model can fit structures associated with all four phases as well as the intermediate structures.

1. Introduction

Small-angle scattering (SAS) data are analyzed either using standard linear plots (such as Guinier or Porod plots) or using nonlinear least-squares fits to appropriate models (Guinier & Fournet, 1955; Glatter & Kratky, 1982; Feigin & Svergun, 1987; Roe, 2000). The first method is easily performed and usually gives good estimates of 'particle' size (radius of gyration) and clues as to the nature of the scattering inhomogeneities through the Porod exponent; a Porod exponent $d = 4$ points to particles with smooth surfaces while $d = 3$ points to very rough surfaces. An exponent $d = 3$ can also point to scattering from 'collapsed' polymer chains (in a bad solvent) and $d = 5/3$ points to scattering from 'fully swollen' chains (in a good solvent). An exponent $d = 2$ can represent scattering either from Gaussian polymer chains or from a two-dimensional structure (such as lamellae or platelets). An exponent $d = 1$ represents scattering from a stiff rod (or thin cylinder). Porod exponents less than 3 are for 'mass fractals' while Porod exponents between 3 and 4 are for 'surface fractals'.

A new Guinier–Porod empirical model is introduced. This model is used to fit actual scattering data from a Pluronic solution that forms the following phases upon heating: unimers with dissolved copolymers, spherical micelles, cylindrical micelles and finally lamellar micelles. This single new model can fit these diverse shapes. Alternative methods to fit the described data would involve the use of four separate models.

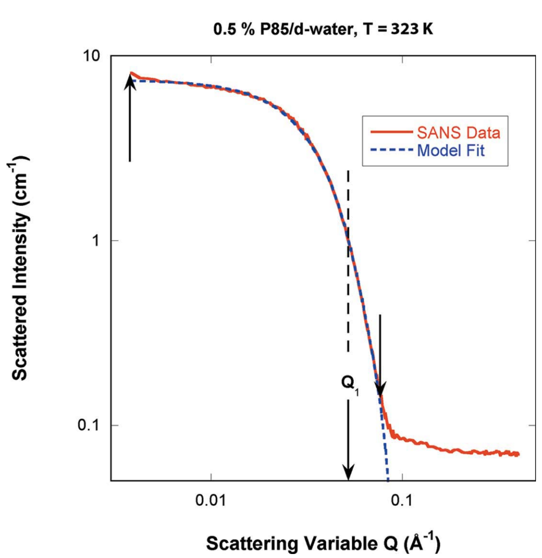

Figure 1
SANS data and fit to the Guinier–Porod model [equations (1) and (2)]. The fitting region is delimited by arrows.

2. The Guinier–Porod model

A Guinier–Porod empirical model is introduced here. The scattering intensity is given by the two contributions

$$I(Q) = G\exp\left(\frac{-Q^2R_g^2}{3}\right) \quad \text{for } Q \le Q_1, \qquad I(Q) = \frac{D}{Q^d} \quad \text{for } Q \ge Q_1. \tag{1}$$

Q is the scattering variable, $I(Q)$ is the scattered intensity, R_g is the radius of gyration, d is the Porod exponent, and G and D are the Guinier and Porod scale factors, respectively. With the requirement that the values of the Guinier and Porod terms and their slopes (derivatives) be continuous at a value Q_1, the following relationships are obtained:

$$Q_1 = \frac{1}{R_g}\left(\frac{3d}{2}\right)^{1/2}, \qquad D = G\exp\left(\frac{-Q_1^2R_g^2}{3}\right)Q_1^d = G\exp\left(-\frac{d}{2}\right)\left(\frac{3d}{2}\right)^{d/2}\frac{1}{R_g^d}. \tag{2}$$

The Guinier form is used for $Q \le Q_1$ and the Porod form is used for $Q \ge Q_1$. The two forms are never used concurrently. Note that the value of Q_1 does not have to be set; it is

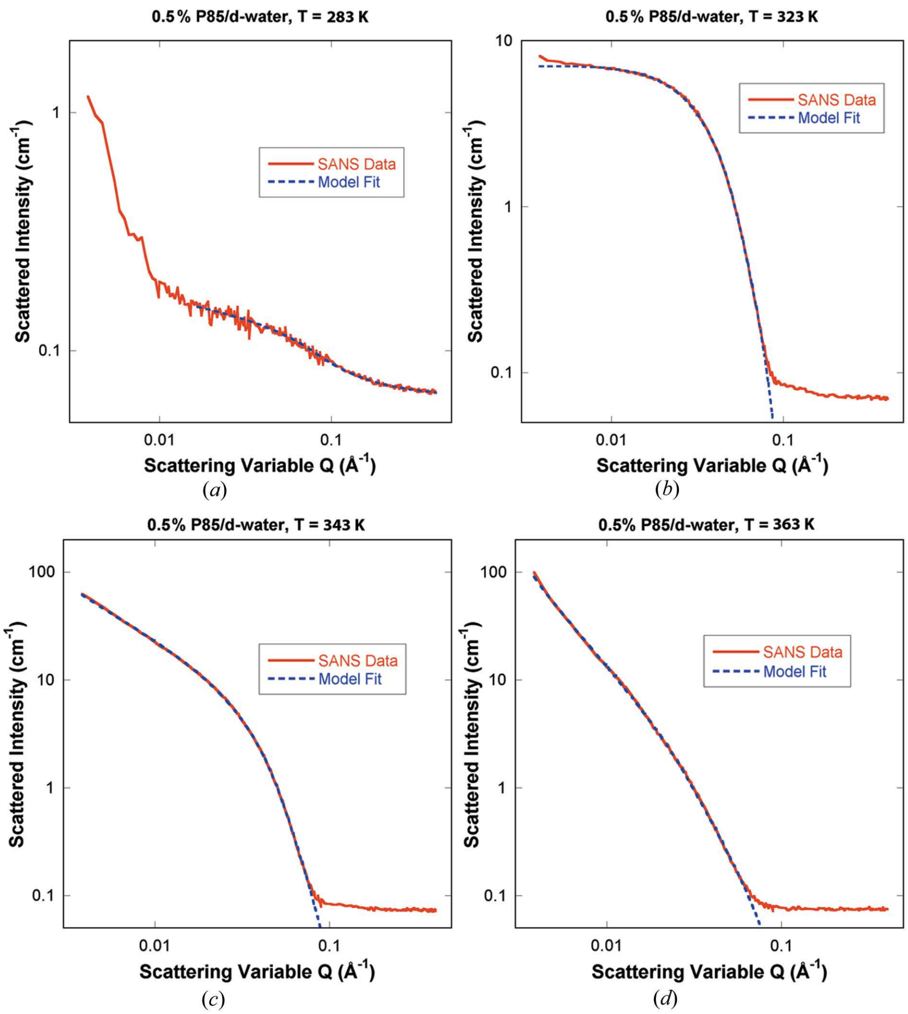

Figure 2
Fits of the generalized Guinier–Porod model to the SANS data from 0.5% P85/d-water at the various temperatures. (*a*) Unimers at 283 K, (*b*) spherical micelles at 323 K, (*c*) cylindrical micelles at 343 K and (*d*) lamellar micelles at 363 K.

calculated internally using equation (2). This model is general and should apply in the entire range of Porod parameters. It is completely empirical. Note that another way of generating the functional form in equation (1) would have been through the use of the Heaviside step function defined as $\Theta(Q-Q_1) = 0$ for $Q < Q_1$ and $\Theta(Q-Q_1) = 1$ for $Q \geq Q_1$. The function $\Theta(Q-Q_1)$ would be multiplying the second term and $\Theta(Q_1-Q)$ would be multiplying the first term. Note also that the Porod exponent d is often a real number.

In order to test the Guinier–Porod model, small-angle neutron scattering (SANS) data from a Pluronic system forming micelles are used. The SANS data were taken at the NIST Center for Neutron Research. The sample temperature was varied from 283 to 363 K. Pluronics are a class of triblock copolymers comprising poly(ethylene oxide) (PEO) and poly(propylene oxide) (PPO) blocks. Pluronic P85 consists of the following block sequence: $EO_{26}PO_{40}EO_{26}$. SANS data taken from 0.5% P85 in a d-water (deuterated water) sample at 323 K are discussed first. P85 is known to form spherical micelles in these conditions. The low P85 fraction was used in order to avoid inter-micelle contributions. The SANS data are shown in Fig. 1. A nonlinear least-squares fit to the smeared Guinier–Porod model is also included. The fit was performed in the Q range from 0.0038 to 0.075 Å^{-1} (marked by arrows in Fig. 1). Using these values and equation (2) the value of the transition point Q_1 turns out to be $Q_1 = 0.053$ Å^{-1} and is marked in Fig. 1.

The best fit to the Guinier–Porod model yields the following results: G = 7.55 (1), R_g = 46.03 (9) Å and d = 3.97 (9). The high-Q background contains contributions from incoherent as well as coherent scattering and is therefore Q dependent. The coherent part has contributions due to the structure of the PEO chains that are anchored on the spherical micelles containing PPO as well as from the higher-order oscillations of the form factor for the spherical micelles.

The so-called Beaucage (1996) model[1] is often used to model SAS data in order to extract a radius of gyration and a Porod exponent. A generalized empirical Guinier–Porod model is introduced next to model the form factor for nonspherical objects.

3. Generalization of the Guinier–Porod model

In order to generalize the Guinier–Porod model to account for nonspherical scattering objects (such as rods or lamellae), the following functional form is used:

$$I(Q) = \frac{G}{Q^s}\exp\left(\frac{-Q^2R_g^2}{3-s}\right) \quad \text{for } Q \leq Q_1,$$
$$I(Q) = \frac{D}{Q^d} \quad \text{for } Q \geq Q_1. \tag{3}$$

This is based on the generalized Guinier law for such elongated objects as rods or lamellae (Luzzati, 1960; Kratky, 1963; Glatter & Kratky, 1982; Hjelm *et al.*, 1992). The same scaling factor G has been kept even though it has different units. The s parameter helps model nonspherical objects. For three-dimensional globular objects (such as spheres), $s = 0$ and one recovers the results of the previous section. For rods $s = 1$ and for lamellae (or platelets) $s = 2$. A dimensionality parameter $3 - s$ is defined.

[1] Equation (8) of Beaucage (1996) relating the Guinier and the Porod scaling factors is in error. It should read $B = (Gd_f/R_g^{d_f})\Gamma(d_f/2)[(6d_f^2)/(2+d_f)\times(2+2d_f)]^{d_f/2}$ instead. Allowing these two factors to float independently during the nonlinear least-squares fitting process produces undesired artifacts.

Table 1
Fits of the Guinier–Porod model to the SANS data.

The reported statistical uncertainties obtained from the fits correspond to one standard deviation. Note that Q_1 is not a fit parameter.

Temperature (K)	G	$3 - s$	R_g (Å)	d	Q_1
283	0.032 (4)	2.75 (3)	15.81 (66)	1.53 (7)	0.096 (5)
323	9.19 (11)	3.000 (3)	46.42 (14)	3.91 (9)	0.0541 (8)
343	0.321 (3)	2.060 (2)	37.10 (14)	4.82 (16)	0.072 (1)
363	0.0036 (1)	1.208 (5)	27.17 (29)	2.87 (1)	0.076 (1)

Applying the same continuity of the Guinier and Porod functions and their derivatives yields

$$
\begin{aligned}
Q_1 &= \frac{1}{R_g}\left[\frac{(d-s)(3-s)}{2}\right]^{1/2}, \\
D &= G\exp\left(\frac{-Q_1^2R_g^2}{3-s}\right)Q_1^{(d-s)} \\
&= \frac{G}{R_g^{(d-s)}}\exp\left[-\frac{(d-s)}{2}\right]\left[\frac{(d-s)(3-s)}{2}\right]^{(d-s)/2}.
\end{aligned} \tag{4}
$$

Note that the factor under the square root must be positive. This means that the constraints $d > s$ and $s < 3$ must be satisfied.

In order to test the generalized Guinier–Porod model, SANS data from the 0.5% P85/d-water sample at different temperatures are analyzed. That sample is known to form unimers (dissolved copolymers in solution) at 283 K, spherical micelles at 323 K, cylindrical micelles at 343 K and lamellar micelles at 363 K. The unimer phase is characterized by scattering from dissolved polymer coils (high Q) and some clustering at low Q. Ideal Gaussian coils give a form factor (the so-called Debye function) which varies as $1/Q^2$ in the Porod region. The form factor for spheres shows a flat low-Q part while the high-Q part dies out as $1/Q^d$ (with $d = 4$ for spheres with smooth surfaces). The form factor for cylinders shows a low-Q part which varies as $1/Q^1$ and a high-Q part that dies out as $1/Q^4$ (for a smooth surface).

Fits of the SANS data to the generalized Guinier–Porod model give reasonable results as shown in Table 1 and Fig. 2. The 'dimensionality' parameter $3 - s$ varies as it should.

Note that the radius of gyration for a sphere of radius R is given by $R_g = R(3/5)^{1/2}$, that for the cross section of a randomly oriented cylinder of radius R is given by $R_g = R/2^{1/2}$, whereas that for the cross section of a randomly oriented lamella of thickness T is given by $R_g = T/12^{1/2}$.

4. Three regions

Note that the SANS data reported here show scattering from very long cylinders (at 343 K) or from extended lamellae (at 363 K). Only the cylinder radius or lamellar thickness can be obtained from the intermediate-Q Guinier region observed (shown in Fig. 3). The data window is limited at low Q so that no low-Q Guinier region can be observed. This low-Q Guinier region would allow an estimate of the cylinder length or lamellar lateral size.

The most general case containing three Guinier regions (that account for three different orthogonal particle sizes) can be described by this model. The simpler case with two Guinier regions is included here:

$$
\begin{aligned}
I(Q) &= \frac{G_2}{Q^{s_2}}\exp\left(\frac{-Q^2R_{g2}^2}{3-s_2}\right) \quad \text{for } Q \le Q_2, \\
I(Q) &= \frac{G_1}{Q^{s_1}}\exp\left(\frac{-Q^2R_{g1}^2}{3-s_1}\right) \quad \text{for } Q_2 \le Q \le Q_1, \\
I(Q) &= \frac{D}{Q^d} \quad \text{for } Q \ge Q_1.
\end{aligned} \tag{5}
$$

Here $3 - s_2$ and $3 - s_1$ are the 'dimensionality' parameters, and R_{g2} and R_{g1} are the radii of gyration for the short and overall sizes of the scattering object. For a cylinder of radius R and length L, $R_{g2} = (L^2/12 + R^2/2)^{1/2}$ and $R_{g1} = R/2^{1/2}$. For a lamella of thickness T and width W, $R_{g2} = (W^2/12 + T^2/12)^{1/2}$ and $R_{g1} = T/12^{1/2}$.

Here also, applying the constraint of continuity of the intensity function (of Q) and its derivative twice yields two transition regions, a new one at Q_2 and the old one at Q_1. Q_2 is between the low-Q and intermediate-Q Guinier regions and Q_1 is between the intermediate-Q Guinier region and the Porod region:

$$
\begin{aligned}
Q_2 &= \left[(s_1 - s_2)\Big/\left(\frac{2}{3-s_2}R_{g2}^2 - \frac{2}{3-s_1}R_{g1}^2\right)\right]^{1/2}, \\
G_2 &= G_1\exp\left[-Q_2^2\left(\frac{R_{g1}^2}{3-s_1} - \frac{R_{g2}^2}{3-s_2}\right)\right]Q_2^{(s_2-s_1)}.
\end{aligned} \tag{6}
$$

During the fitting to the generalized Guinier–Porod model, the first term in equation (5) is used for $Q \le Q_2$, the second term is used for $Q_2 \le Q \le Q_1$ and the third term is used for $Q \ge Q_1$. Here also, keeping the factor under the square root positive implies $3 > s_1 > s_2$ and $R_{g2}^2/(3-s_2) - R_{g1}^2/(3-s_1) > 0$ (*i.e.* $R_{g2} > R_{g1}$).

The case of scattering from a cylinder, for example, is obtained by setting $3 - s_2 = 3$ (*i.e.* $s_2 = 0$) and $3 - s_1 = 2$. The form factor for a cylinder with $G_2 = 1$, $R_{g2} = 100$ Å, $R_{g1} = 10$ Å and $d = 4$ is plotted in Fig. 3. These radii of gyration correspond to a cylinder length $L = 12^{1/2}(100^2 - 10^2)^{1/2} = 344.67$ Å and radius $R = 10(2)^{1/2} = 14.14$ Å. Note that the $1/Q$ region characterizing a long rod applies between the low-Q and the intermediate-Q Guinier regions.

When the form factor given by the Guinier–Porod model contains three regions, it requires that $s_1 \ge s_2$. In general, for scattering objects with spherical symmetry $s_2 = s_1 = 0$ and for cylindrical objects $s_2 = 0$ and $s_1 = 1$. For lamellae with equal width and length, one has $s_2 = 0$ and $s_1 = 2$. Lamellae that are characterized by three distinct sizes (thickness, length and width) would be best described by three Guinier regions and a Porod region (a total of four regions) with $s_3 = 0$ for the lowest-Q Guinier region.

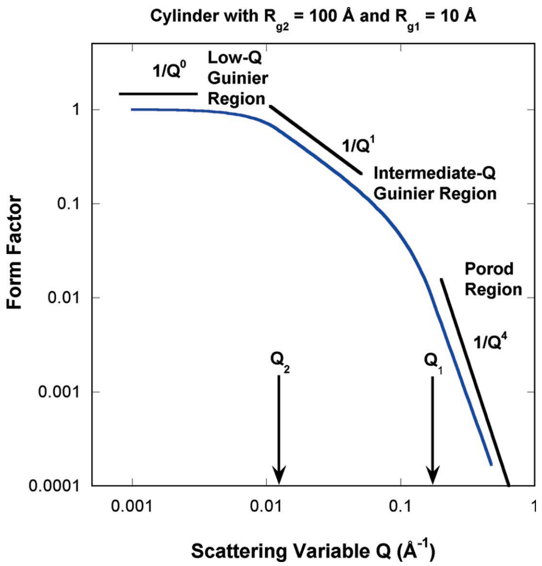

Figure 3
Form factor for a cylinder plotted using the Guinier–Porod model.

5. Discussion

A new Guinier–Porod empirical model has been introduced and applied to scattering from nonspherical objects. Multiple Guinier–Porod regions can be identified. For example, a cylindrical object is characterized by three regions: the high-Q region corresponds to $1/Q^4$, the intermediate-Q region corresponds to $1/Q^1$ and the low-Q region corresponds to $1/Q^0$.

When analyzing SAS patterns from nonspherical objects, clues can yield hints as to the investigated structure. A $1/Q^4$ behavior in the very high Q region points to particles as basic units. A $1/Q^2$ behavior in the very high Q region points to flexible polymer coils. If the $1/Q^2$ behavior is observed at low Q, this usually points to scattering from flat objects (such as lamellae). A simple inspection often determines the number of regions in the scattering window. There are usually three regions: a low-Q Guinier region, an intermediate-Q Guinier region and a high-Q Porod region. If the low-Q window of the spectrometer is restricted, the low-Q Guinier region is not visible. If the scattering objects have three distinct sizes, there could be three Guinier regions and a Porod region instead for a total of four regions. This is the case for lamellae with different thickness, width and length or ellipsoids with three different orthogonal sizes (triaxial ellipsoid).

The single Guinier–Porod model described here can empirically model widely different structures and could provide a simple shortcut for obtaining useful information from the scattering from a nonspherical object. The alternative would be to perform standard linear plots (such as the Guinier or Porod plots). These have limited reliability for complex phase behavior involving diverse particle shapes. The other alternative method would be to use exact known form factors for discrete structures (such as polymer coils, spheres, cylinder, lamellae *etc.*). One would have to use multiple models for each phase structure rather than the single model described here. Moreover, the exact structure factors method does not cover structures intermediate between the known discrete limits: for example, the intermediate structure representing elongated ellipsoids between spheres and cylinders, or the intermediate oblate structure between cylinders and lamellae. The model described here still does not handle peaks in the SAS data in its present form. Peaks could be handled by multiplying the particle form factor described here by a structure factor. Also, this model cannot reproduce oscillations characteristic of form factors for compact monodisperse scattering objects.

The identification of commercial products does not imply endorsement by the National Institute of Standards and Technology nor does it imply that these are the best for the purpose. This work is based upon activities supported in part by the National Science Foundation under agreement No. DMR-0454672. Discussions with David Mildner and Steve Kline are appreciated.

References

Beaucage, G. (1996). *J. Appl. Cryst.* **29**, 134–146.
Feigin, L. A. & Svergun, D. I. (1987). *Structure Analysis by Small-Angle X-ray and Neutron Scattering*. New York: Plenum Press.
Glatter, O. & Kratky, O. (1982). *Small-Angle X-ray Scattering*, ch. 4, pp. 155–156. London: Academic Press.
Guinier, A. & Fournet, G. (1955). *Small-Angle Scattering of X-rays*. New York: John Wiley and Sons.
Hjelm, R. P., Thiyagarajan, P. & Alkan-Onyuksel, H. (1992). *J. Phys. Chem.* **96**, 8653–8661.
Kratky, O. (1963). *Prog. Biophys. Mol. Biol.* **13**, 105–173.
Luzzati, V. (1960). *Acta Cryst.* **13**, 939–945.
Roe, R. J. (2000). *Methods of X-ray and Neutron Scattering in Polymer Science.* New York: Oxford University Press.